

ON THE MASS TRANSFER - ORBITAL PERIOD RELATION IN CATAclySMIC VARIABLES

J. Echevarría

Instituto de Astronomía
Universidad Nacional Autónoma de México

Received 1993 December 8

RESUMEN

Se discute un método simple para calcular tasas de transferencia de masa en variables cataclísmicas. La temperatura $T(R)$ de un disco de acreción en estado estacionario varía como $R^{-3/4}$, lo que lleva a una relación entre la tasa de acreción, el radio externo del disco R_e y la temperatura media del disco, $\dot{M} \propto R_e^3 T_m^4$. Se encuentra que si el radio del disco es una fracción constante de la separación de la binaria entonces $R_e \propto P^{2/3}$ y $\dot{M} \propto T_m^4 P^2$. Basándose en argumentos teóricos y datos observacionales, se muestra que no existe una correlación entre T_m y P , por lo que se concluye que $\dot{M} \propto P^2$. Dado que el radio de la estrella secundaria es función del período orbital, se encuentra que la transferencia de masa es directamente proporcional al área superficial de la compañera: $\dot{M} \propto A_s$. Se hacen estimaciones de T_m a partir de líneas de emisión y de fotometría de Strömgren para calcular tasas de transferencia de masa en una muestra grande de variables cataclísmicas y se comparan los resultados con otros autores.

ABSTRACT

A simple method to obtain mass transfer rates in cataclysmic variables is discussed. The temperature $T(R)$ of a steady accretion disc varies as $R^{-3/4}$, leading to a connection between the accretion rate, the external radius R_e and the mean temperature of the disc, $\dot{M} \propto R_e^3 T_m^4$. We find that if the disc size is a roughly constant fraction of the binary separation then $R_e \propto P^{2/3}$ and $\dot{M} \propto T_m^4 P^2$. We argue from theoretical and observational reasons that there is no correlation between T_m and P , leading to the conclusion that $\dot{M} \propto P^2$. Since the radius of the secondary star is a function of the orbital period, we find that the mass transfer is directly proportional to the surface area of the companion star: $\dot{M} \propto A_s$. We use emission lines and Strömgren photometry to estimate T_m and to calculate mass transfer rates for a large sample of cataclysmic variables, and compare the results with other authors.

Key words: ACCRETION – ACCRETION DISKS — NOVAE – CATAclySMIC VARIABLES

1. INTRODUCTION

Cataclysmic variables are short period semi-detached binaries in which the matter transferred from a late-type secondary star, generally results in an accretion disc around the white dwarf primary star (Warner & Nather 1971). The long term evolution, or secular evolution of these systems will depend on the mechanisms that drive the mass transfer. It is generally thought that angular momentum loss, via gravitational radiation, stellar wind or magnetic braking, is responsible for such drive (see review by Ritter 1986 for detailed references). A comparison of the theoretical predictions

with observed values of the mass transfer rate \dot{M} , will help to understand and establish which processes are occurring. Observables are, however, not easy to derive. Patterson (1984) (hereinafter P84) has reviewed the methods to obtain \dot{M} and has found an $\dot{M} - P$ correlation. Verbunt & Wade (1984) (hereinafter VW84) have published a compilation of mass transfer rates that have been derived from observations. In this paper, we derive a simple new method to obtain \dot{M} , based on the mean temperature of accretion discs, which might be an observable parameter either from observations of emission lines (Echevarría 1988,

hereinafter Paper I) or from broad band photometry (Echevarría, Costero, & Michel 1993, hereinafter Paper II).

2. MASS TRANSFER IN A SEMI-DETACHED BINARY

The mass transfer rate \dot{M} is a fundamental parameter in the accretion disc temperature structure. If we assume that the disc is in LTE then:

$$T(R) = T_* \left\{ \left(\frac{R_w}{R} \right)^3 \left[1 - \left(\frac{R_w}{R} \right)^{1/2} \right] \right\}^{1/4}, \quad (1)$$

where $T_* = (3GM_w\dot{M}/8\pi\sigma R_w^3)^{1/4}$, Pringle (1981), where G is the gravitational constant, M_w and R_w are the mass and radius of the white dwarf, σ is the Stefan-Boltzmann constant and R is the disc radius corresponding to $T(R)$, the temperature emitted at each annulus. We define the mean temperature as

$$T_m = (1/A_{disk}) \int_i^e T(R) dA,$$

i.e., the integral of $T(R)$ weighted by the area of the annuli over the limits i and e , corresponding to the inner R_i and external R_e radius of the disc respectively. Substituting $A_{disk} = \pi R_e^2 - \pi R_i^2$ and $dA = 2\pi R dR$ and taking $T(R)$ from eq. (1) we obtain:

$$T_m = \frac{2T_* R_w^{3/4}}{(R_e^2 - R_i^2)} \int_i^e \left[R - R_w^{1/2} R^{1/2} \right]^{1/4} dR. \quad (2)$$

If we assume that \dot{M} is independent of R , i.e., that \dot{M} is constant throughout the disc and equal to the mass transfer rate, then:

$$\log \dot{M} (\text{g s}^{-1}) = 17.35 - 4 \log \xi + 4 \log \left(\frac{T_m}{10^4} \right) - \log \left(\frac{M_w}{M_\odot} \right), \quad (3)$$

where

$$\xi (\text{cm}^{-3/4} 10^8) = 10^8 / (R_e^2 - R_i^2) \times \int_i^e \left[R - R_w^{1/2} R^{1/2} \right]^{1/4} dR.$$

ξ can be solved numerically, for a given set of R_w , R_i and R_e values. We have made several computations of the integral for a wide range of values. Figure 1 shows some of the results. We find that ξ does not depend strongly on R_w and R_i . For $8.95 \leq \log R_i$ (cm) ≤ 9.99 , $\log \xi$ will vary at most by a factor of 1.6 when $\log R_e$ (cm) = 10.0. For larger outer

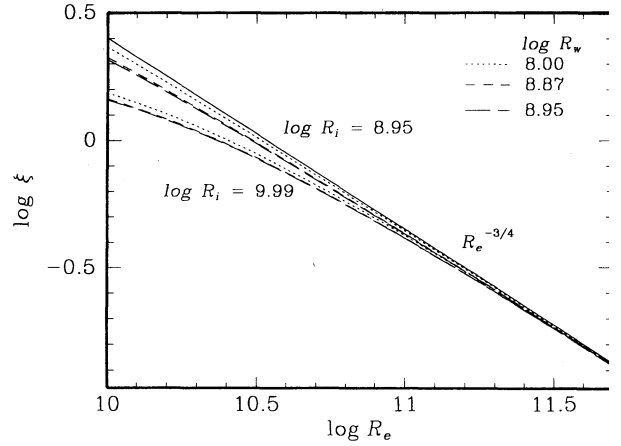


Fig. 1. Numerical calculations of the mass transfer function ξ for a range of inner and outer radii in accretion discs. The straight line is the $R_e^{-3/4}$ approximation.

radii $\log \xi$ is almost independent of R_w and R_i . Therefore $\log \xi$ depends strongly only on R_e . Since $\dot{M} \propto \xi^4$, the results will depend critically on the accurate evaluation of R_e . Note that for $R \gg R_w$, $R - R_w^{1/2} R^{1/2} \approx R$. In this case the integral has a simple analytical solution given by

$$\xi/10^8 = \frac{4}{5} \frac{R_e^{5/4} - R_i^{5/4}}{R_e^2 - R_i^2}, \quad (4)$$

and for $R_e \gg R_i$,

$$\xi/10^8 \approx \frac{4}{5} R_e^{-3/4}. \quad (5)$$

This approximation is shown in Figure 1 as the straight line. The broken lines are the numerical solutions for wide range of values of R_w and R_i . These solutions behave like $R_e^{-3/4}$ for most values of R_e . Thus, we propose an analytical approximation to the integral with the $R_e^{-3/4}$ term, multiplied by a factor of less than unity which accounts for the deviations of ξ at small values of R_e , given by

$$\log \xi = 7.90 - \frac{3}{4} \log R_e + \log \left[1 - 1.15 \left(\frac{R_i R_w}{R_e^2} \right)^{2/5} \right]. \quad (6)$$

The analytical approximations (dashed lines) are compared with the numerical solutions (dotted lines) in Figure 2, for expected minimum and maximum values of R_1 . We use $\log R_w$ (cm) =

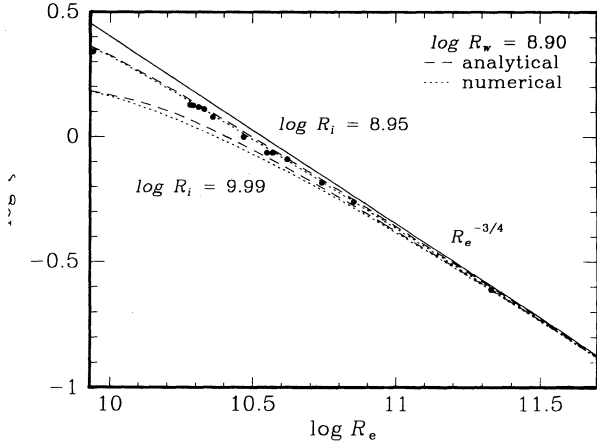


fig. 2. Numerical calculations of the mass transfer function ξ (dotted curves) are compared with the analytical solutions (dashed curves). The straight line is the $R_e^{-3/4}$ approximation.

.90, which is the white dwarf radius mean value of the sample of cataclysmic variables discussed in §3. The analytical solution is in general accurate to 10 percent, except for a combination of low values of R_w and R_e , and high values of R_i . For example, if $\log R_w = 8.00$ and $\log R_i = 9.95$, the solution not shown in the figure) becomes very flat in the range $10.00 \leq \log R_e \leq 10.60$. However, such values are not expected in real systems, i.e., we do not expect to have long orbital period systems with very narrow rings near the white dwarf. In short period systems the inner radius is more likely to be around 10^9 , and in large period systems R_e will be an order of magnitude larger than R_i (see Table 1 for examples). In real systems the analytical approximation will be very satisfactory for all values of R_w .

The mass transfer rate may now be written as

$$\log \dot{M} \text{ (g s}^{-1}\text{)} = 15.74 + 4 \log \left(\frac{T_m}{10^4} \right) + 3 \log \left(\frac{R_e}{10^{10}} \right) - 4 \log \left[1 - 1.15 \left(\frac{R_i R_w}{R_e^2} \right)^{2/5} \right] - \log \left(\frac{M_w}{M_\odot} \right). \quad (7)$$

This equation can be expressed in terms of the orbital period by using the Roche-Lobe, orbital period relationship that holds for all semi-detached binaries. We take the approximation derived by Schevarría (1983) (his eq. (4) modified for the case of the primary star):

$$\left(\frac{R_L}{R_\odot} \right) = 0.2400 \left(\frac{M_w}{M_\odot} \right)^{1/3} P(h)^{2/3},$$

where $P(h)$ is the orbital period in hours.

We substitute $R_w = aR_i$, and $R_e = bR_L$, where a and b are constants, and use the Hamada & Salpeter (1961) mass-radius relation for white dwarfs, assuming that their relation is valid for cataclysmic variables. We take the analytical approximation by Paczynski (1985, private communication in Anderson 1988)

$$\left(\frac{R_w}{R_\odot} \right) = 0.0128 \left(\frac{M_w}{M_\odot} \right) \times \left[1 - \left(\frac{M_w}{1.458 M_\odot} \right)^{4/3} \right]^{0.47} \quad (9)$$

Substituting the above relations into eq. (7) we obtain:

$$\log \dot{M} = 16.41 + 4 \log \left(\frac{T_m}{10^4} \right) + 2 \log P(h) + 3 \log b - 4 \log \left\{ 1 - 0.1102 \frac{a^{-0.4}}{b^{0.8}} \left(\frac{M_w}{M_\odot} \right)^{-8/15} \times \left[1 - \left(\frac{M_w}{1.458 M_\odot} \right)^{4/3} \right]^{0.37} P(h)^{-8/15} \right\}. \quad (10)$$

Of the last three terms, the $2 \log P$ term alone, corresponds to the $R^{-3/4}$ approximation. The other two have opposite signs, with the first one dominating for a combination of very massive white dwarfs, low values of b and values of a approaching unity. In these cases the mass transfer rate could be overestimated by a factor of 10. Since the last term is always greater than zero (otherwise there would be no disc!) it tends to balance the $3 \log b$ term, especially for systems with low mass white dwarfs and small values of a . In the next section we will derive the constants a and b from direct knowledge of R_e , R_i and R_w for a sample of well known cataclysmic variables. We will show there that for most cases we can safely set a and b equal to unity, and have a simplified mass transfer rate relation:

$$\log \dot{M} = 16.41 + 2 \log P(h) + 4 \log \left(\frac{T_m}{10^4} \right). \quad (11)$$

If the mean temperature of accretion discs is not a function of the orbital period, then to a first approximation $\dot{M} \propto P^2$. Since the radius of the secondary star is proportional to the orbital period

(e.g., Echevarría 1983) then the mass transfer rate is directly proportional to the area of the late type star: $\dot{M} \propto A_s$, a very simple, if not surprising result: all things being equal, bigger systems are brighter.

The case that T_m is uncorrelated with P can be made by looking at the results of most theoretical studies (e.g., Williams 1980; Tylenda 1981). The outer temperature does not decrease substantially for bigger discs, but remains essentially constant due to the coolant nature of the emission lines. Broad band photometry of dwarf novae also support our case. For example, Echevarría & Jones (1984) have shown that $(B - V)$ indices of dwarf novae at quiescence increase only as a function of period due to the presence of the secondary stars. This is supported by a more recent study from Strömgren photometry (Paper II).

To obtain mass transfer rates we need to compute T_m from theoretical models or to derive its value from any observational method; for example, emission line ratios or broad band photometry of the disk. This will be discussed in § 4 and 5.

3. DISC PARAMETERS OF SELECTED ECLIPSING SYSTEMS

Mass transfer rates can be derived from eq. (3) if $\log \xi$, T_m and M_w are known. To solve ξ numerically we need to know specific values of R_w , R_i and R_e . The white dwarf radius may be derived from eq. (9) if the mass of the primary is known. The emission lines of eclipsing systems contain information on R_i and R_e . Evidence from spectroscopic observations during the eclipse of high inclination systems (Williams & Ferguson 1982), and from the profiles of the double-peaked emission lines (e.g., Young, Schneider, & Schectman 1981a,b), demonstrates that these lines are formed in the disc. If we use the standard assumption that the rotation of the disc is Keplerian, we obtain R_i and R_e through the relations:

$$\log R_i(\text{cm}) = 16.12 + \log \left(\frac{M_w}{M_\odot} \right) + 2 \log \left(\frac{\sin i}{V_{maz}} \right), \quad (12)$$

and

$$\log R_e(\text{cm}) = \log a + \log \left(\frac{K_r K_w}{V_{min}^2} \right) + \log \left(1 + \frac{K_r}{K_w} \right), \quad (13)$$

where i is the inclination angle of the system, K_r and K_w are the radial velocity semi-amplitudes of the secondary and primary stars respectively, V_{maz} is the maximum velocity in the wings of the emission profile in km s^{-1} , a is the binary separation in cm, and $2V_{min}$ is the separation between the two emission peaks. It has been noted by several authors previously, that in some discs, R_e appears to be larger than the Roche Lobe radius R_L (cf. Young & Schneider 1980; Marsh, Horne, & Shipman 1987). This enlargement may not be real; it is likely that either the emission line semi-amplitudes do not represent the motion of the white dwarf entirely, or that the Keplerian approximation is not accurate for the outer rim of the disc. If R_e exceeds R_L as prescribed in eq. (8) we may use the latter as the upper limit in the integral. Although we are not evaluating the physical limits of the discs, but actually the boundaries of the emission line region these can be produced over more than 80 percent of the disc as we will show in the next section. Only the inner boundary where the temperature is too high for hydrogen to recombine is not taken into account, but this is a very small region.

To obtain estimates of R_i and R_e we need a sample of double-lined, double-peaked eclipsing systems. Such combination is rare among the well observed sample of nearly a hundred objects (e.g. Ritter 1987). In fact the only eclipsing systems with published radial velocity amplitudes and measured peak-to-peak separation are: V363 Aur, AC Cnc, EM Cyg, U Gem and Z Cha, but only the last three have emission line fluxes available from the literature. It is possible, however, to calculate \dot{M} for objects which lack one of the three main ingredients by making additional assumptions. For systems which are not double-lined, K_r may be derived from eclipse modeling; R_e may be substituted by R_i in those cases where the spectrum of the secondary is not visible; and for objects which are not eclipsing it may be possible to derive the inclination angle using a main-sequence mass-radius relation, or the mass and radius for an evolved system.

Table 1 shows the basic parameters for 13 well known cataclysmic variables which comply with the criteria discussed above. These are nine dwarf novae, two classical novae and two nova-like objects. The latter four systems however, have spectroscopic features similar to the dwarf novae. Recent evidence, for example, shows that GK Per itself undergoes dwarf nova outbursts (Szkody 1986) while LX Ser is a VY Scl type system. Thus our results will be biased in the sense that they reflect the conditions prevailing in dwarf novae. We have included only 3 systems which are not eclipsing. These are: GK Per, AE Aqr and AH Her. The inclination of GK Per has been derived from a analysis of the evolution of a low-mass giant and

TABLE 1

BASIC PARAMETERS OF WELL KNOWN
CATACLYSMIC VARIABLES

name	$\log P$ (h)	V_{min} (km s ⁻¹)	V_{maz} (km s ⁻¹)	i (°)	K_w (km s ⁻¹)	K_r (km s ⁻¹)	$\log a$	$\log R_w$	$\log R_i$	$\log R_e$	$\log R_L$	M_w (M_\odot)	Ref. ^a
K Per	1.681	175	1000	63 ^b	34	124	11.69	8.81	9.97	11.49	11.33	0.90	1
E Aqr	0.995	...	1800	64 ^b	135	159	11.27	8.85	9.43	...	10.85	0.82	2
M Cyg	0.844	390	1900	63	170	135	11.15	8.97	9.21	10.57	10.70	0.56	3
H Her	0.792	300	1300	46 ^b	126	158	11.16	8.79	9.58	10.86	10.74	0.95	4
Q Her	0.667	330	1200	80	136	192 ^c	10.96	9.02	9.60	10.72	10.55	0.45	5
Gem	0.628	564	2500	67	137	284	11.04	8.64	9.32	10.62	10.66	1.18	6,7
X Ser	0.580	...	1550	75	162	185 ^c	10.90	9.04	9.31	...	10.47	0.40	8
W Sex	0.510	630	1830	79	144	253 ^c	10.88	8.96	9.35	10.28	10.48	0.58	9
Cha	0.252	600	2100	82	64	430	10.71	8.84	9.40	10.48	10.36	0.84	10,11
T Cas	0.247	597	2820	81	58	388 ^c	10.66	8.94	9.00	10.34	10.31	0.61	12,13
X Hya	0.214	650	3500	78	69	414 ^c	10.68	8.87	8.91	10.34	10.33	0.78	14
Y Car	0.191	684	2100	83	45	439 ^c	10.64	8.91	9.31	10.34	10.29	0.68	13,15
2051 Oph	0.176	808	2150	81	91	350 ^c	10.58	9.03	9.08	9.94	10.22	0.43	16

References: (1) Crampton, Cowley, & Fisher 1986; (2) Chincarini & Walker 1981; (3) Stover, Robinson, & Nather 1981; (4) Horne, Wade, & Szkody 1986; (5) Young & Schneider 1980; (6) Stover 1981; (7) Wade 1981; (8) Young, Schneider, & Schectman 1981a; (9) Penning et al. 1984; (10) Marsh, Horne, & Shipman 1987; (11) Wade & Horne 1988; (12) Young, Schneider, & Schectman 1981b; (13) Wood 1987; (14) Hellier et al. 1987; (15) Bailey & Ward 1981; (16) Watts et al. 1986.

Derived from mass-radius relation.

Derived from eclipse analysis.

compact object (Crampton, Cowley, & Fisher 1986). Although the inclination derived by these authors is 63°, and therefore a small deviation will not affect $a \sin i$ strongly, we must consider this system with extreme caution because it has the largest disc and the largest orbital period in the sample. The measurement of $2V_{min}$ is uncertain because of the separation of the peaks in the emission line is small and the line profiles are variable. Thus, we may have in this case, a large error in ξ and consequently in R_e . The calculations of ξ for the sample are shown in Table 2 and depicted in Figure 2. We observe that the points are closer to the calculations for $\log R_i = 8.95$ (In fact the mean $\log R_i$ value of the sample is $\log R_i = 9.34$), and not very far from the $R^{-3/4}$ approximation. Thus it seems not too unreasonable to use eq. (11) for those systems without knowledge of the disc parameters, provided we can produce an estimate of the mean temperature.

To finish this section, it is convenient to complete our discussion on how valid is the $a = b = 1$ approximation, as this yields the simplified eq. (11). We can test this assumption with the 13 systems discussed above, which have the best known disc parameters, by plotting in Figure 3, as a function of orbital period: the b parameter, the $C_0 = a^{-0.4}/b^{0.8}$ term in eq. (10) and the fraction of

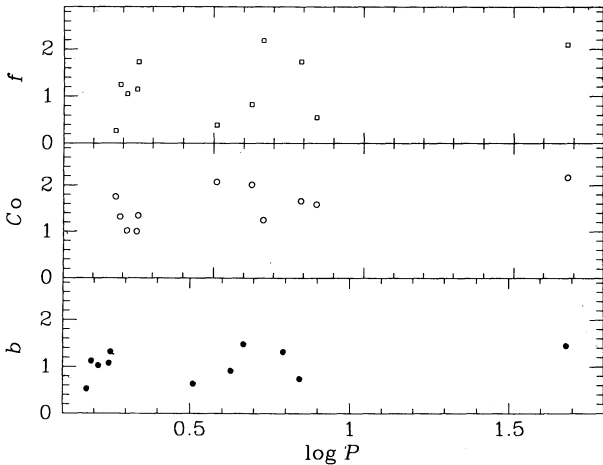


Fig. 3. Disc parameters for the best known systems as a function of orbital period: the b parameter (lower), the $C_0 = a^{-0.4}/b^{0.8}$ ratio (middle) and the filling factor $f = (b^2 - (c/a)^2)/(1 - c^2)$, where $R_w = cR_L$ (upper).

disc area with respect to the total available area, $f = (b^2 - (c/a)^2)/(1 - c^2)$, where $R_w = cR_L$. The derived b and f values greater than unity correspond to the case where we are measuring bigger outer disc radii than Roche-Lobe radii, and as discussed before this may be due to the outer

rim failure to follow a Keplerian orbit or that the radial velocity semi-amplitudes are distorted by asymmetric components. Note that the f ratio is dominated completely by the b parameter. There are only four systems with b less than unity, with values of 0.74, 0.69, 0.63 and 0.52. In these extreme cases the last two terms in eq. (10) would decrease the mass transfer rate only by a factor of 1.8, 2.34, 2.14 and 2.51 respectively. The C_0 coefficient varies between 1 and 2 and does not modify substantially the last term in eq. (10). We conclude therefore, that in general eq. (11) is a good approximation.

4. MASS TRANSFER RATES FROM EMISSION LINES

Obtaining disc temperatures from emission line ratios might be a very unreliable process, since the lines might be formed only in the external parts of the disc, where they are the main coolant. In this case we will observe a kinetic temperature of the external parts which is essentially constant (≈ 6000 K). Similarly, if the lines are formed in a photoionized region above the disc, the line temperature is likely to be fixed at a value close to 10^4 K. There are, however, many examples of cataclysmic variables whose Balmer lines present very broad wings indicating large velocities which can only be explained if they are formed at the inner parts of the disc. Moreover, the line ratios in many of these objects have values which follow very simple LTE calculations for a series of uniform layers of hydrogen at high densities (Paper I). It is also important to know what range of T_m values we should expect. Figure 4 shows the mean temperature as a function of external disc radius for different mass transfer rates. These are derived from eq. (3) using the ξ numerical integrations, with $\log R_w = 8.90$, $\log R_i = 8.95$ and assuming $\log M_w = 0$. Only for very large mass transfer rates the mean temperature rises above 30 000 K. For $\log \dot{M} < 16$ it falls below 10 000 K for all values of R_e . The reason for this behaviour is simply that the lower temperatures in the disc dominate because they are produced at much larger areas than the inner high temperature rings. For example, if we take the above M_w , R_w and R_i values with $\log \dot{M} = 17.0$ and $\log R_e = 10.6$ we obtain $T_m = 7370$ K. Following eq. (1) the internal and external temperatures are 35 360 K and 4055 K respectively, but 80 percent of the disc will be below 12 810 K. Thus, the emission lines can be produced in most of the disc and at moderate temperatures.

A statistical analysis of the emission lines of 69 cataclysmic variables has been made in Paper I from data available from the literature. It is shown there that the $H\delta/H\beta$ and $He\ I\ 4471/H\beta$ ratios are strongly correlated with $H\gamma/H\beta$. A

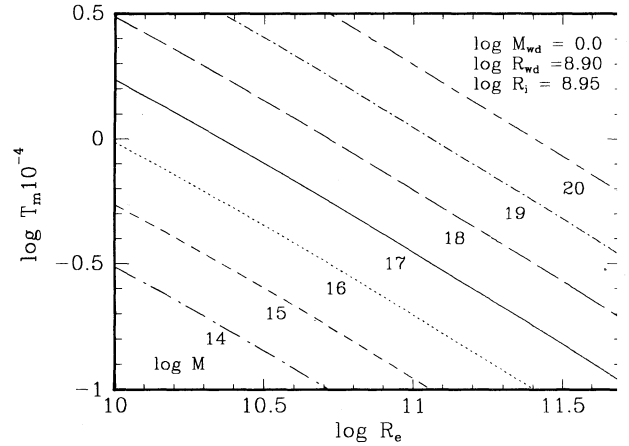


Fig. 4. Mean temperature as a function of external disc radius for different mass transfer rates, using the ξ numerical integrations, for $\log R_w = 8.90$, $\log R_i = 8.95$ and $\log M_w = 0$.

comparison with the line ratios calculated by Drake & Ulrich (1980) for a high density uniform slab of hydrogen indicates that the Balmer decrement of cataclysmic variables is a function of the mean temperature in the emitting region. Quite clearly accretion discs are not a slab of uniform density at the same temperature, but we may think then as a series of uniform density rings at different temperatures. This collection of rings will show a mean temperature value, and this is what we could use to obtain estimates of \dot{M} .

We can take the case of a Doppler line profile given by

$$\frac{H\gamma}{H\beta} = 1.57 \frac{\exp(29599/T_m) - 1}{\exp(33153/T_m) - 1}, \quad (14)$$

and

$$\frac{H\delta}{H\beta} = 1.97 \frac{\exp(29599/T_m) - 1}{\exp(35085/T_m) - 1}, \quad (15)$$

(adapted from Drake & Ulrich 1980).

The emission line ratios were taken from the compilation in Paper I. Line intensities $I(\lambda)$, corrected for interstellar absorption were calculated from the relation

$$\log I(\lambda)/I(H\beta) = \log F(\lambda)/F(H\beta) + C(H\beta)f(\lambda), \quad (16)$$

where $F(\lambda)$ is the observed flux, $C(H\beta)$ is the logarithmic reddening correction at $H\beta$ and $f(\lambda)$ is the reddening function normalized at $H\beta$, derived

TABLE 2

EMISSION LINE RATIOS AND CORRECTIONS, MEAN TEMPERATURES, ξ VALUES AND MASS TRANSFER RATES FOR WELL KNOWN CATACLYSMIC VARIABLES^a

Name	EW						T_m		$\log \xi$	$\log \dot{M}$ (g s^{-1})	
	(H β)	$F_{\text{H}\gamma}$	$F_{\text{H}\delta}$	$C_{\text{H}\beta}$	$I_{\text{H}\gamma}$	$I_{\text{H}\delta}$	H γ	H δ		H γ	H δ
GK Per	11	0.85	0.57	0.32	0.94	0.66	7000	5000	-0.612	19.22	18.64
AE Aqr	47	0.72	...	0.06	0.73	...	4650	...	-0.260	17.15	...
AE Aqr	22	0.85	0.39	0.06	0.87	0.40	6000	3450	-0.260	17.59	16.63
AE Aqr	50	0.85	0.69	0.06	0.87	0.71	6000	5400	-0.260	17.59	17.40
EM Cyg	3	1.15	...	0.07	1.19	...	14500	...	-0.064	18.50	...
EM Cyg	11	0.96	...	0.07	0.98	...	7700	...	-0.064	17.40	...
AH Her	24	0.90	...	0.04	0.91	...	6600	...	-0.184	17.39	...
AH Her	26	0.84	0.82	0.04	0.85	0.84	5800	6500	-0.184	17.16	17.36
DQ Her	33	0.64	0.44	0.15	0.67	0.47	4150	3800	-0.064	16.43	16.27
DQ Her	17	0.71	0.65	0.15	0.74	0.70	4700	5300	-0.064	16.64	16.85
DQ Her	20	0.62	0.67	0.15	0.65	0.72	4000	5450	-0.064	16.36	16.90
U Gem	15	0.85	0.81	0.04	0.86	0.83	5900	6400	-0.090	16.72	16.86
LX Ser	26	0.85	0.80	0.14	0.89	0.85	6300	6600	-0.001	16.95	17.03
SW Sex	...	0.86	0.93	0.09	0.88	0.97	6200	7900	0.127	16.25	16.67
Z Cha	26	0.60	0.67	0.06	0.61	0.69	3750	5200	0.078	15.41	15.98
HT Cas	77	0.56	0.40	0.08	0.57	0.42	3500	3550	0.118	15.27	15.29
HT Cas	98	0.89	0.84	0.08	0.91	0.87	6600	6800	0.118	16.37	16.42
HT Cas	117	0.82	0.71	0.08	0.84	0.74	5700	5600	0.118	16.11	16.08
EX Hya	74	0.65	...	0.05	0.66	...	4100	...	0.110	15.47	...
OY Car	34	0.66	0.39	0.05	0.67	0.40	4150	3450	0.125	15.49	15.17
V2051 Oph	124	0.72	0.55	0.07	0.74	0.57	4700	4400	0.340	15.04	14.93

^a Observed fluxes and corrected intensities are relative to H β . The observed values are from the compilation in Paper I.

om the normal extinction law (Whitford 1958). alues of $C(\text{H}\beta)$ where obtained mainly from the ompilation by Warner (1988) or from other sources ere $E(B - V)$ excesses and/or distances are given. The mean temperatures derived from these atios are given in Table 2. No correlation between n and P was found. The mean value from the mple is: $T_m = 5636 \pm 1941$ K. This value is nsistent with what we should expect as discussed ove.

Mass transfer can now be estimated from eq. (3) sing the caluated ξ , M_w and T_m values. The sults are shown in the last two columns of Table 2. [$\log \dot{M}$, $\log P(h)$] diagram is depicted in Figure 5 r the mean value from both line ratios. The raight lines correspond to eq. (11), for $T_m = 10^4$ K ottered) and for $T_m = 5700$ K (solid). The dot-long ashed curve corresponds to P84 relation $\log \dot{M} = 1.58 + 3.2 \log P(h)$.

We find that in general, there is good agreement etween the individual points calculated from the ll solution in eq. (3) and the simplified solution eq. (11). Note that the only observation during

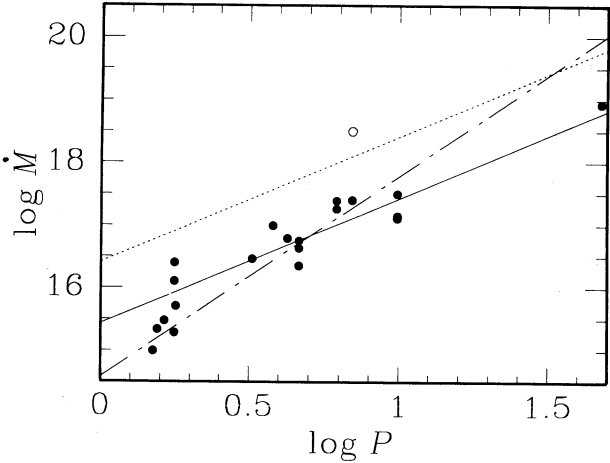


Fig. 5. Mass transfer rates as a function of orbital period for well known cataclysmic variables. The points are taken from Table 2. The open circle corresponds to EM Cyg in outburst (see text). The solutions correspond to eq. 11), for $T_m = 10^4$ K (dotted line) and for $T_m = 5700$ K (solid line). The dot-long dashed curve corresponds to P84 relation.

TABLE 3
EMISSION LINE RATIOS AND CORRECTIONS, MEAN TEMPERATURES, AND
MASS TRANSFER RATES FOR OTHER CATAclysmic VARIABLES^a

Name	log <i>P</i> (h)	EW (Hβ)						<i>T_m</i>		log <i>Ṁ</i> (g s ⁻¹)	
			<i>F_{Hγ}</i>	<i>F_{Hδ}</i>	<i>C_{Hβ}</i>	<i>I_{Hγ}</i>	<i>I_{Hδ}</i>	Hγ	Hδ	Hγ	Hδ
V Sge	1.091	62	0.59	0.42	0.22	0.63	0.46	3900	3800	16.96	16.91
V Sge	1.091	53	0.71	0.43	0.22	0.76	0.48	4900	3900	17.35	16.96
V Sge	1.091	62	0.57	0.42	0.22	0.61	0.46	3750	3800	16.89	16.91
V Sge	1.091	61	0.56	0.65	0.22	0.60	0.72	3700	5500	16.86	17.55
SY Cnc	0.960	9	1.28	0.72	:0.2	1.36	0.79	>5E4	6000	>21.00	17.44
SY Cnc	0.960	14	1.19	1.13	:0.2	1.27	1.24	22000	13000	19.70	18.79
SY Cnc	0.960	14	1.34	0.90	:0.2	1.43	0.99	>5E4	8100	>21.00	17.96
RU Peg	0.954	4	1.02	0.45	0.08	1.05	0.47	9100	3850	18.15	16.66
RU Peg	0.954	5	0.98	0.66	0.08	1.00	0.68	8000	5200	17.93	17.18
RU Peg	0.954	16	1.19	1.49	0.08	1.22	1.55	16300	43000	19.17	20.85
RU Peg	0.954	28	0.72	...	0.08	0.74	...	4700	...	17.01	...
CH UMa	0.918	35	1.02	0.80	0.05	1.04	0.82	8800	6300	18.02	17.44
BT Mon	0.904	23	0.75	0.74	0.29	0.82	0.85	5500	6600	17.18	17.50
BT Mon	0.904	22	0.57	0.67	0.29	0.62	0.67	3800	5100	16.54	17.05
BT Mon	0.904	35	0.61	0.64	0.29	0.67	0.73	4150	5500	16.69	17.18
BT Mon	0.904	31	0.68	0.70	0.29	0.74	0.80	4700	6100	16.91	17.36
BT Mon	0.904	13	0.37	...	0.29	0.40	...	2600	...	15.88	...
Z Cam	0.842	34	0.44	...	0.08	0.45	...	2850	...	15.91	...
Z Cam	0.842	5	0.52	0.44	0.08	0.53	0.46	3300	3800	16.17	16.41
V426 Oph	0.836	15	0.74	0.70	0.09	0.76	0.73	4900	5500	16.84	17.04
V426 Oph	0.836	18	0.93	0.71	0.09	0.96	0.74	7300	5600	17.54	17.07
V533 Her	0.830	5	0.98	0.45	0.11	1.01	0.47	8100	3800	17.70	16.39
SS Cyg	0.820	40	0.81	0.74	0.06	0.83	0.76	5600	5800	17.04	17.10
SS Cyg	0.820	74	0.80	...	0.06	0.82	...	5500	...	17.01	...
SS Cyg	0.820	70	0.76	0.66	0.06	0.77	0.68	5000	5150	16.85	16.90
SS Cyg	0.820	67	0.76	0.57	0.06	0.77	0.59	5000	4550	16.85	16.68
SS Cyg	0.820	30	1.08	1.02	0.06	1.10	1.05	10500	9000	18.13	17.87
SS Cyg	0.820	32	0.98	0.49	0.06	1.00	0.50	8000	4000	17.66	16.46
SS Cyg	0.820	25	1.17	1.35	0.06	1.19	1.39	14500	19500	18.70	19.21
RX And	0.706	58	1.01	0.77	0.06	1.03	0.79	8600	6000	17.56	16.93
SS Aur	0.642	58	0.72	0.53	0.15	0.75	0.57	4800	4400	16.42	16.27
SS Aur	0.642	76	0.89	...	0.15	0.93	...	6800	...	17.02	...
SS Aur	0.642	95	0.84	0.73	0.15	0.88	0.78	6200	5950	16.86	16.79
SS Aur	0.642	106	0.82	0.67	0.15	0.86	0.72	5900	5450	16.78	16.64
SS Aur	0.642	122	0.85	0.58	0.15	0.89	0.62	6300	4750	16.89	16.40
TW Vir	0.642	78	0.92	0.75	0.20	0.98	0.82	7600	6300	17.22	16.89
TW Vir	0.642	14	0.89	0.73	0.20	0.95	0.80	7200	6100	17.12	16.84
TW Vir	0.642	70	0.73	0.60	0.20	0.78	0.66	5100	5000	16.52	16.49
TW Vir	0.642	96	0.85	0.78	0.20	0.90	0.86	6400	6700	16.92	17.00
TW Vir	0.642	73	1.05	0.99	0.20	1.12	1.09	11000	9600	17.86	17.62
WW Cet	0.625	62	0.98	...	0.09	1.01	...	8200	...	17.32	...
WW Cet	0.625	43	0.95	0.93	0.09	0.98	0.97	7700	7900	17.21	17.25
WW Cet	0.625	25	0.99	0.65	0.09	1.02	0.68	8400	5200	17.36	16.52
WW Cet	0.625	18	1.14	1.09	0.09	1.17	1.14	13500	10500	18.18	17.74
FO Aqr	0.605	25	0.67	0.74	0.13	0.70	0.79	4400	6000	16.19	16.73
FO Aqr	0.605	27	0.82	0.62	0.13	0.85	0.66	5800	5000	16.67	16.42
FO Aqr	0.605	17	0.82	0.47	0.13	0.85	0.50	5800	4000	16.67	16.03
FO Aqr	0.605	19	0.52	0.60	0.13	0.54	0.64	3350	4900	15.72	16.38
DO Dra	0.600	...	0.84	0.73	0.05	0.85	0.75	5800	5700	16.66	16.63

TABLE 3 (CONTINUED)

Name	log <i>P</i>	EW						<i>T_m</i>		log \dot{M} (g s ⁻¹)	
	(h)	(H β)	<i>F_{Hγ}</i>	<i>F_{Hδ}</i>	<i>C_{Hβ}</i>	<i>I_{Hγ}</i>	<i>I_{Hδ}</i>	H γ	H δ	H γ	H δ
DO Dra	0.600	129	0.65	0.51	0.05	0.66	0.52	4100	4100	16.06	16.06
X Leo	0.596	41	0.70	...	0.16	0.74	...	4700	...	16.29	...
X Leo	0.596	22	0.80	0.95	0.16	0.84	1.02	5700	8500	16.63	17.32
CM Del	0.590	16	0.61	0.41	0.12	0.63	0.43	3900	3600	15.95	15.82
CM Del	0.590	23	0.63	0.39	0.12	0.65	0.41	4000	3500	16.00	15.77
V380 Oph	0.584	9	1.00	...	0.05	1.02	...	8300	...	17.25	...
AB Dra	0.562	33	1.06	1.14	0.15	1.11	1.22	10800	12300	17.67	17.89
AB Dra	0.562	20	0.86	0.54	0.15	0.90	0.58	6500	4500	16.79	16.15
AB Dra	0.562	20	0.89	0.90	0.15	0.93	0.96	6800	7700	16.86	17.08
V425 Cas	0.555	14	1.65	0.68	0.05	1.68	0.70	>5E4	5300	>21.00	16.42
V425 Cas	0.555	10	3.13	0.68	0.05	3.18	0.70	>5E4	5300	>21.00	16.42
V425 Cas	0.555	9	1.00	0.86	0.05	1.02	0.88	8500	6900	17.24	16.88
V425 Cas	0.555	9	1.82	0.30	0.05	1.85	0.31	>5E4	2950	>21.00	15.40
UU Aql	0.528	50	0.91	0.67	0.05	0.92	0.69	6700	5250	16.77	16.35
UU Aql	0.528	81	0.67	0.42	0.05	0.68	0.43	4200	3600	15.96	15.69
V603 Aql	0.521	8	1.10	0.98	0.10	1.13	1.03	11500	8600	17.69	17.19
V603 Aql	0.521	8	0.87	0.53	0.10	0.90	0.55	6500	4300	16.70	15.99
V603 Aql	0.521	6	1.06	0.48	0.10	1.09	0.50	10200	4000	17.49	15.86
V603 Aql	0.521	5	0.89	0.96	0.10	0.92	1.01	6700	8400	16.76	17.15
TT Ari	0.519	39	0.66	0.53	0.07	0.67	0.55	4150	4300	15.92	15.98
TT Ari	0.519	23	1.01	0.70	0.07	1.03	0.72	8600	5500	17.19	16.41
TT Ari	0.519	10	0.69	0.65	0.07	0.71	0.67	4500	5100	16.06	16.28
TT Ari	0.519	7	0.63	0.49	0.07	0.64	0.51	3950	4050	15.83	15.88
1030+590	0.514	...	0.95	0.98	0.05	0.96	1.00	7300	8200	16.89	17.09
MV Lyr	0.506	29	0.63	0.49	0.15	0.66	0.53	4100	4200	15.87	15.91
MV Lyr	0.506	45	0.88	0.72	0.15	0.92	0.77	6700	5850	16.73	16.49
AR And	0.352	39	0.43	0.70	0.05	0.44	0.72	2800	5500	14.90	16.08
AR And	0.352	39	0.91	0.42	0.05	0.92	0.43	6700	3600	16.42	15.34
AR And	0.352	50	0.71	0.66	0.05	0.72	0.68	4550	5150	15.75	15.96
AR And	0.352	53	0.89	0.71	0.05	0.90	0.73	6500	5550	16.37	16.09
YZ Cnc	0.317	80	0.89	0.76	0.13	0.93	0.81	6800	6200	16.37	16.21
YZ Cnc	0.317	131	0.83	0.71	0.13	0.86	0.75	5900	5700	16.13	16.07
YZ Cnc	0.317	42	1.01	0.97	0.13	1.05	1.03	9100	8700	16.88	16.80
YZ Cnc	0.317	92	0.77	...	0.13	0.80	...	5300	...	15.94	...
SU UMa	0.263	54	1.08	1.14	0.13	1.12	1.21	11200	12100	17.13	17.27
SU UMa	0.263	54	1.04	0.91	0.13	1.08	0.97	9900	7800	16.92	16.50
VW Vul	0.244	114	0.90	0.90	0.22	0.96	1.00	7300	8200	16.35	16.55
VW Vul	0.244	36	0.82	0.81	0.22	0.88	0.90	6200	7100	16.07	16.30
VW Vul	0.244	48	0.80	0.74	0.22	0.86	0.82	5900	6300	15.98	16.10
VW Vul	0.244	38	1.00	0.87	0.22	1.07	0.96	9600	7800	16.83	16.47
IR Gem	0.215	116	0.77	0.63	0.11	0.80	0.66	5300	5000	15.74	15.64
IR Gem	0.215	81	1.08	0.87	0.11	1.12	0.92	11200	7300	17.04	16.29
T Leo	0.150	132	0.82	0.74	0.05	0.83	0.76	5600	5800	15.70	15.76
T Leo	0.150	62	0.75	0.72	0.05	0.76	0.74	4900	5600	15.47	15.70
T Leo	0.150	165	0.67	...	0.05	0.68	...	4250	...	15.22	...
T Leo	0.150	115	0.65	0.53	0.05	0.66	0.54	4100	4250	15.16	15.22
AF Cam	0.100	32	0.72	0.48	0.05	0.73	0.49	4650	3950	15.28	15.00
AF Cam	0.100	33	0.69	0.43	0.05	0.70	0.44	4400	3650	15.18	14.86
AF Cam	0.100	25	0.87	0.68	0.05	0.88	0.70	6200	5300	15.78	15.51

^a Observed fluxes and corrected intensities are relative to H β . The observed values are from the compilation in Paper I.

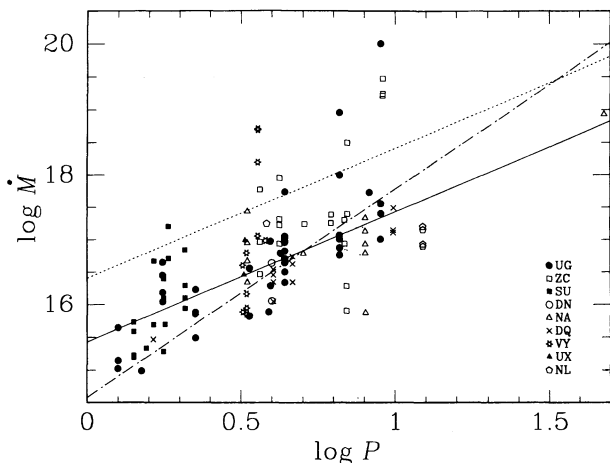


Fig. 6. Mass transfer rates for cataclysmic variables with known orbital periods and emission line ratios, taken from Table 3. The points from Table 2 are also included. The lines have the same meaning as in Figure 5.

outburst from the sample (open circle) has a much larger mass transfer rate. This observation correspond to EM Cyg (Williams 1983) and was taken 3 to 4 days after maximum, when the dwarf nova was still very bright at $V = 12.5$ (Mattei 1981). Compare this with the quiescent observation taken by Oke & Wade (1982) at $V = 13.6$, which has a mass transfer rate down by a factor of 13.

Mass transfer rates were calculated for other cataclysmic variables for which there are no observable disc parameters, but have observed emission line ratios, using eq. (11). Thirty two cataclysmic variables with emission line ratios were also selected from the compilation in Paper I. The mean temperatures derived from these ratios and the calculated mass transfer rates for the objects are given in Table 3. A $\log \dot{M}$, $\log P(h)$ diagram is shown in Figure 6, for the mean value from both line ratios. The objects in the previous figure have been included. For the two cases where $H\gamma/H\beta$ gives a temperature too high with respect to $H\delta/H\beta$, i.e., $T > 50\,000$ K, we have plotted \dot{M} for the last ratio only. These are observations of SY Cnc and V425 Cas, which show unusually strong lines and large Balmer line ratios. The mass transfer rates from both ratios agree well with each other as shown in Figure 7, however there is, in general, a trend to obtain lower rates from $H\delta/H\beta$ by a factor of 2.4. This difference is independent of subclass but tends to increase with orbital period.

5. MASS TRANSFER FROM STRÖMGREN PHOTOMETRY

Another possible way to obtain mean temperatures is to use broad-band photometry of the disc

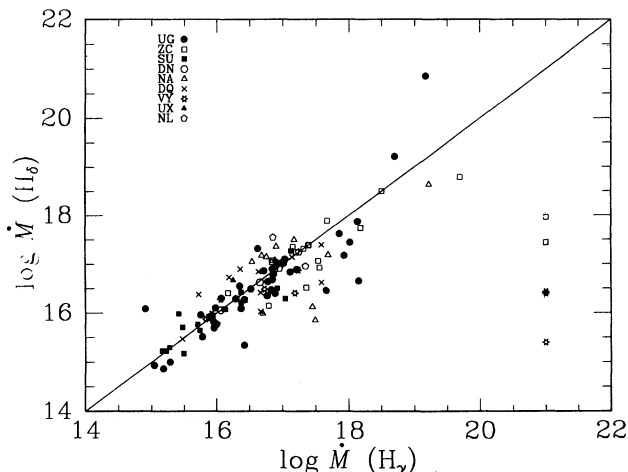


Fig. 7. Comparison of the mass transfer rates from the emission line ratios. The points are taken from the last two columns of Table 2 and 3, and are separated by subclass. The points to the lower and right part of the diagram are only limits.

continuum. As a first step we must find a relation between Strömgren $b-y$ index and T_m , either from disc models or assuming a particular function. Such relation might be substituted in eq. (11) leaving the mass transfer rate as a function of two observable parameters; P and $b-y$.

Figure 8 shows the Strömgren $b-y$ index for dwarf novae at minimum as a function of orbital period. The $b-y$ index is a measure of the disc continuum temperature only since it is not affected by emission lines. The filled circles are systems for which there is spectroscopic evidence of the secondary stars. The orbital period of EY Cyg has been revised to 0.30 days (Echevarría et al. 1994).

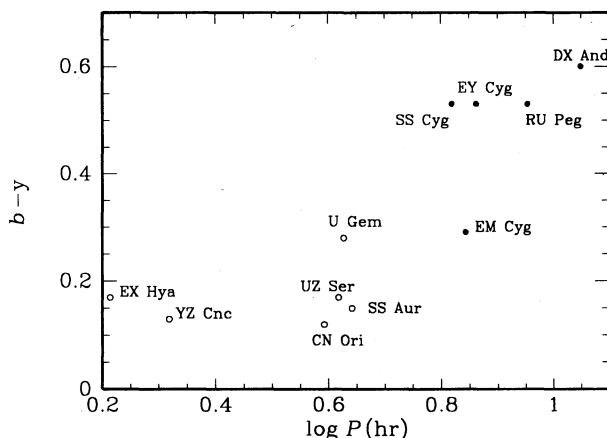


Fig. 8. Orbital period–Strömgren $b-y$ index relation for some dwarf novae. Filled circles are systems with bright secondaries in the visible range.

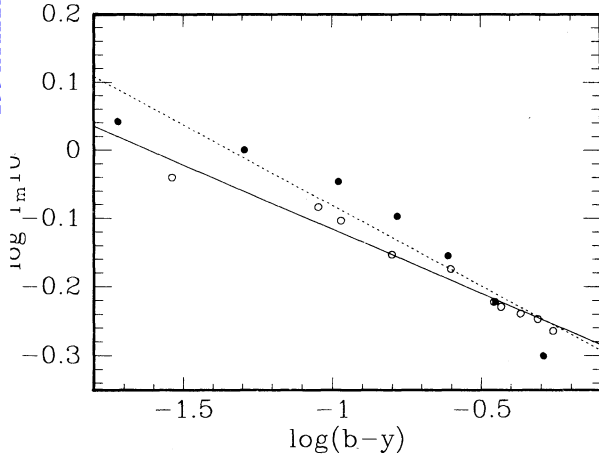


fig. 9. $b - y$ colors and mean temperatures for blackbodies (filled circles) and main sequence stars (open circles). The logarithmic fits give $A = -0.303$ and $B = -0.187$ (dotted line for blackbody) and $A = -0.316$ and $B = -0.236$ (solid line for main sequence). Calculations are limited to a range $0.0 < b - y < 0.6$.

There is no evidence of a disc temperature increase with orbital period. Only the systems with bright secondaries show an increase in $b - y$. The $b - y$ photometry sets an upper limit to the maximum mean temperature we should expect for dwarf novae, i.e., $b - y = 0.1$ for systems at quiescence and $b - y = 0.0$ for systems at maximum (Paper II).

As a first step we have calculated the $b - y$ colors for a blackbody as function of temperature. The appropriate flux intervals were folded with the filter transmissions. The absolute flux density for $m = 0$ was derived from the Vega flux calibration by Hayes & Latham (1975) folding the response of the b and y filters. The results are: $\log F_b = -8.25$ and $\log F_y = -8.45$, with F_λ in $\text{erg cm}^{-2} \text{s}^{-1} \text{\AA}^{-1}$. Figure 9 shows the temperature as a function of $b - y$ index (stars). We propose a logarithmic relation of the form $\log T_m/10^4 = A + B \log(b - y)$. A mean square fit to the data give $A = -0.303$ and $B = -0.187$. This fit is shown in Fig. 9 as a dotted line. This result is compared with $b - y$ and T_m values for main sequence stars (open circles) (Crawford 1975, 1979; Olsen 1984; Johnson 1966) which give $A = -0.316$ and $B = -0.236$. This is shown in Fig. 9 as a solid line. In both cases we have limited the calculations to a range $0.0 < b - y < 0.6$, which is the observable range in cataclysmic variables (Paper II). Following from eq. (11) we obtain:

$$\log \dot{M} = 15.20 + 2 \log P(h) - 0.75 \log(b - y), \quad (17)$$

or a blackbody approximation, and

$$\log \dot{M} = 15.14 + 2 \log P(h) - 0.94 \log(b - y), \quad (18)$$

or a main sequence approximation.

It would be desirable to have a $b - y$, T_m relation directly from accretion disc models, but unfortunately these parameters are not included in any published model. However, since the standard model assumes an LTE condition, the results used here are not altogether unreasonable. We will use the blackbody approximation to derive mass transfer rates. This will give slightly lower values than the main sequence approximation.

Mass transfer rates from eq. (17) are shown in Table 4 for a number of dwarf novae observed in Paper II, and for an unpublished observation of GK Per. The mean value of T_m for systems at quiescence is $T_m(\text{mean}) = 6241 \pm 608$ K. This is, within the errors, similar to the mean value obtained from the emission line ratios in the eclipsing systems.

The results are also depicted in Figure 10. We have included several systems for which the $b - y$ is contaminated from the presence of the secondary star. The real disc value will be substantially lower and therefore in these cases \dot{M} will be a lower limit. The most extreme case is DX And. If we take, for example a disc value of $b - y = 0.4$ then $\log \dot{M}$ will increase to 17.61. It is interesting to note the case of SS Aur and YZ Cnc for which no secondary is present. In both cases the observations cover quiescent and outburst values. The mass transfer in SS Aur increases by a factor of 6.6 over a 4 mag increase during the rise, and for YZ Cnc it increases by a factor of 17.8 over 3 mag between minimum and maximum states.

6. COMPARISON WITH OTHER MASS TRANSFER ESTIMATES AND CONCLUSIONS

P84 has found a relation between the equivalent width of the emission lines and the absolute mag-

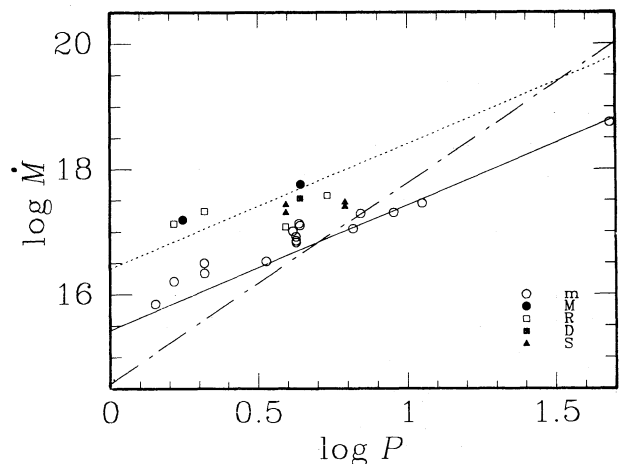


Fig. 10. Mass transfer rates for cataclysmic variables with known orbital periods and Strömgren photometry. The lines have the same meaning as in Figure 5.

TABLE 4

MASS TRANSFER RATES DERIVED FROM EQS.(17) AND (18)
FROM STRÖMGREN PHOTOMETRY OF DWARF NOVAE

Object	<i>y</i>	<i>b - y</i>	<i>T_m</i>	$\log \dot{M}$ (g s^{-1})	$\log P$ (h)	Type	State
GK Per	12.77	0.57	5529	18.75	1.681	NA	m
DX And	15.00	0.60	5476	17.46	1.049	UG	m
RU Peg	12.81	0.53	5605	17.31	0.954	UG	m
EY Cyg	14.79	0.53	5605	17.13	0.86:	UG	m
EM Cyg	13.16	0.29	6274	17.29	0.844	ZC	m
SS Cyg	11.70	0.53	5605	17.05	0.820	UG	m
AH Her	12.55	0.12	7399	17.47	0.792	ZC	S
AH Her	12.77	0.15	7097	17.40	0.792	ZC	S
BV Pup	13.99	0.06	8423	17.58	0.73:	UG	R
SS Aur	14.97	0.15	7097	17.10	0.642	UG	m
SS Aur	10.99	0.02	10344	17.76	0.642	UG	R
SS Aur	11.11	0.02	10344	17.76	0.642	UG	M
TW Vir	13.12	0.04	9087	17.53	0.641	UG	D
U Gem	14.19	0.24	6500	16.92	0.628	UG	m
U Gem	14.59	0.32	6159	16.83	0.628	UG	m
U Gem	13.84	0.29	6274	16.86	0.628	UG	m
UZ Ser	16.23	0.17	6933	17.01	0.618	UG	m
CN Ori	14.10	0.12	7399	17.08	0.593	ZC	R
CN Ori	12.91	0.06	8423	17.30	0.593	ZC	S
CN Ori	12.66	0.04	9087	17.43	0.593	ZC	S
UU Aql	16.52	0.43	5828	16.53	0.53:	UG	m
YZ Cnc	13.47	0.13	7289	16.50	0.317	SU	m
YZ Cnc	15.17	0.21	6664	16.34	0.317	SU	m
YZ Cnc	12.13	0.01	11776	17.33	0.317	SU	R
AY Lyr	13.20	0.01	11776	17.19	0.246	UG	M
IR Gem	12.79	0.01	11766	17.13	0.215	SU	R
EX Hya	13.95	0.17	6933	16.21	0.214	DQ	m
FS Aur	15.94	0.34	6090	15.85	0.15:	UG	m

nitude of the discs, using the latter to interpolate Tytenda (1981) disc models to obtain \dot{M} . VW84 have published a compilation of mass transfer rates that have been derived from observations by a number of methods. A direct comparison for the thirty three objects in common with P84 and eighteen in common with VW84 are shown in Figure 11. For these common samples we find mean $\log \dot{M}$ values of 16.98 (VW84), 16.49 (P84) and 16.94 (this paper), while a least squares fit gives: $\log \dot{M} = 15.29 + 1.87 \log P$ for P84 and $\log \dot{M} = 16.93 + 0.07 \log P$ for VW84, compared with $\log \dot{M} = 15.66 + 1.90 \log P$ for our crossed sample. This last result is obvious since our data have been calculated using eqs. (3) or (11). What is striking is that the mean values are similar, and in particular that the

fit in the P84 sample is very close to our $\dot{M} \propto P$ result. The data in P84 is based on a completely independent observable parameter, and the fact that both methods give similar results is very encouraging. The data in VW84 contain more objects in a high state or in outburst than the data in P84 and in this paper. This is due to the fact that emission lines are observed in quiescence or low states. Only a few objects have been taken near maximum with the Strömgren photometry, and these systems show clearly that the mass transfer rate increases substantially during outburst. Mass transfer rate estimates for V2051 Oph, OY Car, FO Aqr and V533 Her are nearly the same as P84 but in cases like GK Per, V Sge, AE Aqr or BT Mon the results differ substantially. It is possible that in some cases we are comparing different accretive

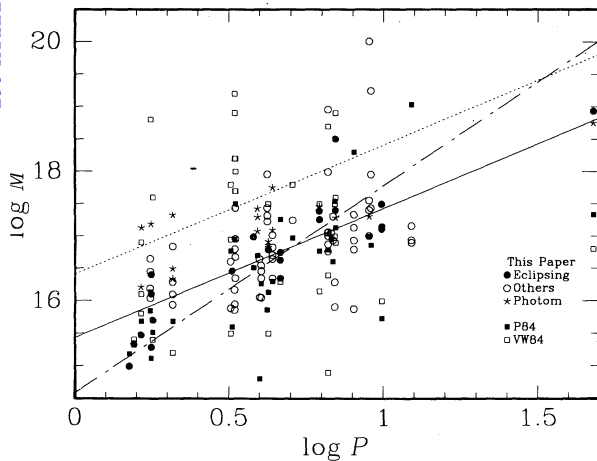


fig. 11. Mass transfer rates derived from observations by different methods and authors. A direct comparison is made for thirty three objects in common with P84 and eighteen in common with the compilation by VW84.

disc states like in TT Ari, where the top two points were observed during a high state (Wargau et al. 1982), while the rest were obtained at a low state.

In conclusion we find our results are not only compatible with other methods, but also that our analytical solution permits the calculation of a larger sample of cataclysmic variables in all states, provided we have emission line ratios or $b - y$ photometry. We encourage people who work on detailed disc modelling to include calculations of τ_m and $b - y$ as well as emission and absorption line ratios to improve some of the assumptions made in this work and to be able to obtain more accurate mass transfer rates.

I would like to thank J. Cantó and J. Bohigas for fruitful discussions and suggestions on several aspects of this work, and to the Royal Society and the Academia de la Investigación Científica in México for their generous support.

REFERENCES

- Anderson, N. 1988, *ApJ*, 325, 266
 Bailey, J., & Ward, M. 1981, *MNRAS*, 194, 17
 Chincarini, G., & Walker, M.F. 1981, *A&A*, 104, 24
 Cramppton, D., Cowley, A.P., & Fisher, W.A. 1986, *ApJ*, 300, 788
 Crawford, D.L. 1975, *AJ*, 80, 955
 ———. 1979, *AJ*, 84, 1858
 Drake, S.A., & Ulrich, R.K. 1980, *ApJS*, 42, 351
 Echevarría, J. 1983, *RevMexAA*, 8, 109
 Echevarría, J. 1988, *MNRAS*, 233, 531 (Paper I)
 Echevarría, J., & Jones, D.H.P. 1984, *MNRAS*, 206, 919
 Echevarría, J., Costero, R., & Michel, R. 1993, *A&A*, 275, 201 (Paper II)
 Echevarría, J., Arrieta, A., Olguín, L., & Vázquez, R. 1994, in preparation
 Hamada, T., & Salpeter, E.E. 1961, *ApJ*, 134, 683
 Hayes, D.S., & Latham, D.W. 1975, *ApJ*, 197, 593
 Hellier, C., Mason, K.O., Rosen, S.R., & Córdova, F.A. 1987, *MNRAS*, 228, 463
 Horne, K., Wade, R.A., & Szkody, P. 1986, *MNRAS*, 219, 791
 Johnson, H.L. 1966, *ARA&A*, 4, 193
 Marsh, T.R., Horne, K., & Shipman, H.L. 1987, *MNRAS*, 225, 551
 Mattei, J., 1981, AAVSO, private communication
 Oke, J.B., & Wade, R. 1982, *AJ*, 87, 670
 Olsen, E.H. 1984, *A&AS*, 57, 443
 Patterson, J. 1984, *ApJS*, 54, 443
 Penning, W.R., Ferguson, D.H., McGraw, J.T., Liebert, J., & Green, R.F. 1984, *ApJ*, 276, 233
 Pringle, J.E. 1981, *ARA&A*, 19, 137
 Ritter, H. 1986, in *The Evolution of Galactic X-Ray Binaries*, ed. J. Trümper, W.H.G. Lewin, & W. Brinkmann, NATO ASI Series C., Vol. 167 (Dordrecht: Reidel), p. 271
 ———. 1987, *A&AS*, 70, 335
 Stover, R.J. 1981, *ApJ*, 248, 684
 Stover, R.J., Robinson, E.L., & Nather, R.E. 1981, *ApJ*, 248, 696
 Szkody, P. 1986, *ApJ*, 301, L29
 Tylenda, R. 1981, *Acta Astron.*, 31, 127
 Verbunt, F., & Wade, R. 1984, *A&AS*, 57, 193
 Wade, R.A. 1981, *ApJ*, 246, 215
 Wade, R.A., & Horne, K. 1988, *ApJ*, 324, 411
 Wargau, W., Drechsel, H., Rahe, J., & Vogt, N. 1982, *A&A*, 110, 281
 Warner, B., & Nather, R.E. 1971, *MNRAS*, 152, 219
 Warner, B. 1988, *MNRAS*, 227, 23
 Watts, D.J., Bailey, J., Hill, P.W., Greenhill, J.G., McCowage, C., & Carly, T. 1986, *A&A*, 154, 197
 Whitford, A.E. 1958, *AJ*, 63, 201
 Williams, G. 1983, *A&AS*, 53, 323
 Williams, R.E. 1980, *ApJ*, 235, 939
 Williams, R.E., & Ferguson, D.H. 1982, *ApJ*, 257, 672
 Wood, J. 1987, *Ap&SS*, 130, 81
 Young, P., & Schneider, D.P. 1980, *ApJ*, 238, 955
 Young, P., Schneider, D.P., & Sheckman, S.A. 1981a, *ApJ*, 244, 259
 ———. 1981b, *ApJ*, 245, 1035

Juan Echevarría: Instituto de Astronomía, UNAM, Apartado Postal 877, 22860 Ensenada, B.C., México.
 E-mail: jer@bufadora.astrosen.unam.mx.